IEEE Access
Multidisciplinary | Rapid Review | Open Access Journal

Received February 18, 2020, accepted March 1, 2020, date of publication March 5, 2020, date of current version March 17, 2020.

Digital Object Identifier 10.1109/ACCESS.2020.2978663

A Practical Calibration Method of Linear UHF Yagi Arrays for Ship Target Detection Application

CAIJUN WANG, YINGWEI TIAN, (Member, IEEE), JING YANG, HAO ZHOU, (Senior Member, IEEE), BIYANG WEN, AND YIDONG HOU

Radar and Signal Processing Laboratory (RSPL), Electronic Information School, Wuhan University, Wuhan 430072, China

Corresponding author: Caijun Wang (wcj@whu.edu.cn)

This work was supported in part by the National Natural Science Foundation of China under Grant 41706200 and Grant 61671331, and in part by the National Key Research and Development Program of China under Grant 2017YFC0405703.

ABSTRACT Practical and stable channel calibration method is one of the most interesting technology for array radar engineers. This paper proposes a single source active calibration method (SAM) for ultra high frequency (UHF) radar with uniform linear array (ULA) Yagi antennas. This SAM measures the amplitude and phase errors of receiving channel at a known direction of arrival (DOA) in the antenna pattern measurement (APM) mode of radar without a transponder, then the calibration values at other angles are determined by a formula derived from array signal model. The results of simulation and field experiment show that (1) the antenna pattern (AP) caculated from SAM calibration is consistent with the simulated and measured AP of the Yagi array. (2) after calibrated by SAM values, DOA estimantion of digital beamforming (DBF) and signal to noise ratio (SNR) gains of Doppler power for 5 ship targets are in good agreement with the theoretical performance of 8 arrays. and (3) the azimuth angle of the single active source is insignificant and can be user-defined according to the field environment. It is proved that the proposed SAM calibration provides a feasibility and idea for the practical and reliable calibration of UHF Yagi ULA.

INDEX TERMS Single active calibration method, DOA, DBF, UHF radar, Yagi Array, ULA, ship target detection.

I. INTRODUCTION

The practical and stable receiving channel calibration method is always a difficult problem for the long-term operational running of radar system. Almost all the high resolution spatial spectrum estimation algorithms are based on the accurate knowledge of the antenna array factor, however, in field operating, the antenna array inevitably contains a variety of errors, such as receiving channel amplitude and phase errors, mutual coupling of array elements, position errors of array elements and antenna pattern errors etc., which will seriously degrade the performance of the algorithms and even make them invalid [1], [2]. Over the past decades, a variety of channel calibration methods have been studied and tested for high frequency/ultra-high frequency (HF/UHF) oceanographic radars, including self-calibration (or passive calibration) and active calibration. Self-calibration is of greatest interest because it can be automatically calibrated online, which usually requires joint estimation of the azimuth of the spatial source and the perturbation parameters of the array, based on some optimal cost function. Some special and independent signals on the radar Doppler spectrum are first used for calibration, such as echoes from stationary islands or lighthouses in front of the radar, echoes from non-cooperative ships and so on [3], [4]. Sea clutter is the most used self-calibrating source, because sea echoes are always present, and of course, the single angle of arrival echoes are expected. In recent years, some self-calibration methods based on antenna characteristics and numerical analysis have been proposed and proved to be effective [5], [6]. Furthermore, the automatic identification system (AIS) transmissions from passing vessels which provide the position and bearing to the vessel demonstrate the potentiality in passive calibration. The automatic calibration by associating the ship

The associate editor coordinating the review of this manuscript and approving it for publication was Shah Nawaz Burokur.

echoes in the radar Doppler spectra with the known AIS informations is proved to be a low-cost and steady calibration procedure [7]–[9]. Active calibration is a traditional and practical technology which estimates the array perturbation parameters offline by setting one or more auxiliary sources with known direction of arrival (DOA). Transponder paired with radar system is the most commonly used auxiliary source and is a standard instrument for omnidirectional antenna pattern measurements (APM) in field operating [10]. General radio frequency (RF) signal sources are also optional [11], which are asynchronous with the radar system. A small fishing boat several kilometers away from radar are usually needed for a standard APM procedure to carry the transponder moving in circular arcs around the radar because many radar sites do not have enough land to perform a walking APM [10]. Drone aircraft was successfully conducted to measure APM in recent years at much lower cost and in a broader range of sea states comparing with a boat [12]–[14].

Recently, a UHF radar was developed by RSPL of Wuhan University, China, for ocean remote sensing in coastal zone [15], which uses an 8-element Yagi uniform linear array (ULA) for receiving channel. The UHF radar is designed with a maximum detection distance of 5 km and a range resolution of 10 m. It has potential applications in port navigation, waterfall monitoring of coastal tourist areas and offshore search and rescue. The Yagi antenna was chosen as the receiving element because it provides additional directional gain and reduces the impact of the external environment. For the UHF oceanographic radar application, AIS is not available because most of small boats in the coastal zone are not equipped with it. It's difficult to calibrate passively a ULA because a unique solution of DOA is not guaranteed for the Vandermonde feature of the antenna array factor [16], so the self-calibration methods, mostly eigenstructure-based methods, are usually applied for a nonlinear array [17], [18]. Although some self-calibration algorithms for ULA are numerically simulated to resolve the phase ambiguity problem by imposing some constraints [19]–[22], it's hard to be used in field operating for limited conditions. Helzel and Kniephoff introduced a self-calibration algorithm for linear phased array (PA) and any kind of irregular array of WERA HF radar, in which a normalization of antenna gain is applied by summing up the Bragg-scattered energy from range $2-50$ km for each antenna separately [23]. Hou *et al.* proposed a ULA self-calibration method for UHF radar based on the characteristics of river echo signals (e.g., single flow direction along the river) [24]. Kim *et al.* utilized the radar returns containing the clutter and the opportunity targets to estimate the array error of an active ULA using the phase gradient characteristics of the active ULAs [25]. Active calibration is commonly used for the ULA, and numerical examples show that only partly calibrated sensors are required [26], [27]. Yang *et al.* showed the beampattern of a hydrophone ULA in a lake, with one pair of consecutive hydrophone sensors being calibrated beforehand [28].

In this paper, a single source active calibration method (SAM) is proposed for UHF Yagi ULA calibration, which measures the amplitude and phase errors of receiving channel at only one known DOA. The calibration values at other azimuth angles are determined by a formula derived from signal model. Both computer simulation and field experiment are performed to verify the effectiveness of the proposed method. Existing passive self-calibration method for a ULA is limited to some specific characteristics which may cause unstable application in field operation of radar. As an active calibration method, the SAM is completely controlled and inherently stable for the practical application. In addition, by choosing any convenient angle near the radar site according to the field environment, a practical and reliable calibration procedure can be implemented by SAM method which can reduce sea state limitation or eliminate more labor-intensive alternatives, e.g., operating a boat or unmanned aerial vehicle (UAV) moving in circular arcs around the radar. Furthermore, the UHF radar is designed with two working modes, the operating mode and the APM mode, and the SAM method is carried out in the latter mode of radar by setting parameters of active source such as waveform, distance and power through the system soft of radar, which further simplify the calibration procedure and cost, e.g., eliminating the requirements of a special designed transponder or RF signal generator. In Section II, the SAM calibration procedure is explained in detail based on the array signal model. In Section III, the antenna pattern of Yagi ULA is simulated and measured, and calculated based on SAM calibration, then the effectiveness of SAM is evaluated. The experiment analysis is conducted in Section IV to verify the SAM performance of DOA estimation and signal to noise ratio (SNR) gains of Doppler power for ship target detecion. Section V contains a brief conclusion.

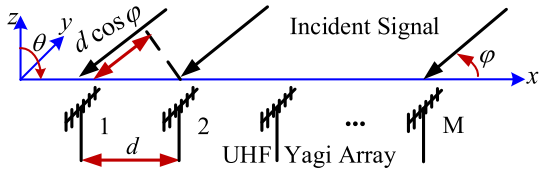

FIGURE 1. Signal model of Yagi ULA.

II. SINGLE ACTIVE CALIBRATION METHOD

The UHF radar was designed as a multi-channel system using digital beamforming (DBF) technology to estimate DOA of target. A ULA of eight UHF Yagi antennas were deployed on the shore for improving azimuth resolution, as shown in Fig. 1. The ULA is along the x-axis, and the vertically polarized Yagi antenna points to the y-axis, or the normal direction of the array. The phase differences of the array are determined by the elevation angle θ and the azimuthal angle φ, which are defined $\theta = 0$ at z-axis, clockwise, and $\varphi = 0$ at x-axis, counterclockwise, respectively.

For Q single and independent DOA signals at the far field, the received signal model of M Yagi array elements can be

described by,

$$\mathbf{X}(t) = F(\theta, \varphi)\Gamma\mathbf{A}(\theta, \varphi)\mathbf{S}(t) + \mathbf{N}(t) \tag{1}$$

where $\mathbf{X}(t)$ is a $M \times 1$ dimensional vector of observation data, $\mathbf{S}(t)$ is the $Q \times 1$ dimensional vector of incident signal, and $\mathbf{N}(t)$ is the $M \times 1$ dimensional vector of Gauss white noise, which is assumed to be independent of $\mathbf{S}(t)$. Γ is a diagonal matrix representing amplitude and phase errors of the multi-channel array and $\mathbf{A}(\theta, \varphi)$ is the array factor of $M \times Q$ dimension matrix, which are given by

$$\begin{aligned} \Gamma &= \mathrm{diag}(1, \Gamma_2 e^{j\gamma_2}, \cdots, \Gamma_M e^{j\gamma_M}) \\ \mathbf{A} &= [\mathbf{a}(\theta, \varphi_1), \mathbf{a}(\theta, \varphi_2), \cdots, \mathbf{a}(\theta, \varphi_Q)] \end{aligned} \tag{2}$$

where Γ_M and γ_M denotes the amplitude and phase error of the M-th receiving channel, respectively, assuming that the first antenna channel is the reference channel. Here we assume that array errors are mainly caused by receiving channel errors, e.g., circuit board errors of receiver, transmission errors of cables and antennas, and the position errors and mutual coupling of array elements are ignored. At elevation angel $\theta = \pi/2$, that is, on the xy-plane, $\mathbf{a}(\pi/2, \varphi) = [1, e^{jkd\cos\varphi}, \cdots, e^{jk(M-1)d\cos\varphi}]^T$ is the ideal steering factor detemined only by the azimuth angle φ, in which $k = 2\pi/\lambda$ is radar wavenumber, λ is the wavelength of radar, $d = \lambda/2$ is the spacing of array element and $[.]^T$ denotes transpose operation. The radiation factor F of a single Yagi antenna is common to all receiving channels, that is, assuming no distortion in Yagi antenna pattern, i.e., Γ is independent of azimuth angle of the incident signal, which is reasonable for UHF Yagi antenna, because of its short wavelength, directional gain, and most interference signals being considered to be in the far field of the antenna. We can obtain

$$F(\theta, \varphi) = \sum_{p=1}^{K}[\frac{2I_p}{k}\frac{\cos(kh_p\cos\theta) - \cos(kh_p)}{\sin(kh_p)\sin^2\theta} \times e^{jky_p\sin\theta\cos(\varphi-\pi/2)}] \tag{3}$$

where we assume that there are K dipoles of the Yagi antenna, with the first and second element being the reflector and driven respectively, and the last $K-2$ being the directors. The maximum gain of Yagi is towards endfire, or towards the normal direction of the ULA, i.e., $\varphi = \pi/2$. p is the index of element, and y_p is the distance of the p-th dipole along the y-axis. h_p is half of the lenght l of the p-th dipole, i.e., $h_p = l/2$, $kh_p = \pi l_p$, where $l_p = l/\lambda$ is the normalized length by radar wavelength. The input currents $\mathbf{I} = [I_1, I_2, \cdots, I_p]^T$ can be computed by $\mathbf{I} = \mathbf{Z}^{-1}\mathbf{V}$, where the input voltages is $\mathbf{V} = [0, 1, 0, \cdots, 0]^T$, and the mutual impedance matrix $\mathbf{Z}$ depends only on the geometry of the dipoles. At elevation angel $\theta = \pi/2$, that is, on the xy-plane, $F(\pi/2, \varphi)$ is detemined only by the azimuthal angle φ, and is constant to all receiving channels for single DOA signal, which does not affect the calibration value of different channel. According to the array pattern multiplication property [29], the Yagi array's total normalized gain g_{tot} at x-y plane will be,

$$g_{tot}(\varphi) = |\sum_{m=1}^{M} e^{jk(m-1)d\cos\varphi}|^2 \times |\sum_{p=1}^{K} I_p \frac{1-\cos(\pi l_p)}{\sin(\pi l_p)} e^{jky_p\cos(\varphi-\pi/2)}|^2 \tag{4}$$

In (1), the amplitude and phase error diagonal matrix Γ of the multi-channel receiver should be estimated before the DBF algorithm is applied. The covariance matrix $\mathbf{R_X}$ of observation data is

$$\mathbf{R_X} = E[\mathbf{X}\mathbf{X}^\mathbf{H}] = |F|^2\Gamma\mathbf{A}R_S\mathbf{A}^H\Gamma^H + \sigma_N^2\mathbf{I} \tag{5}$$

where $E[.]$ and $[.]^H$ denote the expectation and conjugate tranpose operation, respectively. σ_N^2 is the covariance of noise. $\mathbf{R_S} = \mathrm{diag}(|S_1|^2, |S_2|^2, \cdots, |S_Q|^2)$ is the covariance matrix of signal, assuming that the Q incident signals are independent. $\mathbf{I}$ is an identity matrix. Carrying out eigenvalue decomposition of $\mathbf{R_X}$ to separate signal and noise subspace, we obtain eigenvector matrix of signal, $\mathbf{e_S} = [\mathbf{e_1}, \mathbf{e_2}, \cdots, \mathbf{e_Q}]$, which corresponds to the first Q maximum eigenvalues. Base on the theory of spatial spectrum estimation [30], $\mathbf{e_S}$ spans the signal subspace, which is the same space with $\Gamma\mathbf{A}$, that is

$$\Gamma\mathbf{A} = c\mathbf{e_S} \tag{6}$$

where c is an unknown complex constant. Since Γ is independent of the azimuth angle of incident signal, Γ can actually be estimated repeatly Q times by using (6).

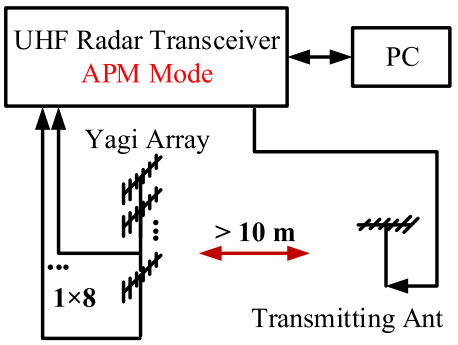

FIGURE 2. APM schematic of radar receiver.

In this paper, to simplify the field operations of radar, a practical calibration method for UHF Yagi ULA called single source active calibration method (SAM) is proposed, in which an active transmitting signal at single azimuth angle is deployed to estimate Γ. Fig. 2 showed a schematic of APM mode of radar receiver, in which mode, radar usually transmitted a single frequency signal or linear frequency modulation (LFM) continuous wave signal instead of the linear frequency modulated interrupting continuous wave (FMICW) in normal operating mode. The transmitting antenna points to the receiving array, and the distance

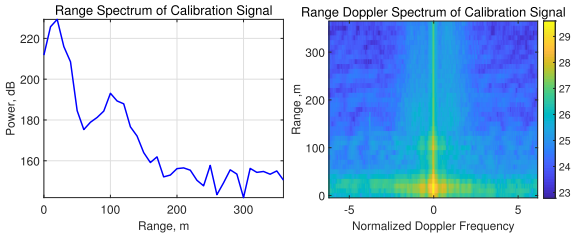

(a) Range Spectrum (b) Range-Doppler Spec

FIGURE 3. Calibration source from range and Doppler spectrum.

between them should be more than 10 times of the wavelength, e.g., > 10 m. The distance and azimuth angle φ_S of the auxiliary active source were controlled manually according to the site environment and recorded by a personal computer (PC) in which the signal frequency (and waveform, if required) and power were set.

Substituting φ_S and $Q = 1$ into (6), it can be written

$$\Gamma_i e^{j\gamma_i} e^{jk(i-1)d\cos\varphi_S} = ce_{1i}, \quad i = 2, 3, \cdots, M \tag{7}$$

where $\mathbf{e_1} = [e_{11}, e_{12}, \cdots, e_{1M}]$ is the eigenvector corresponding to the maximum eigenvalues, and $ce_{11} = 1$. The calibration value of the i-th channel at the azimuth angle φ_S, $C(\varphi_S, i)$, which should be compensated before DBF is used to compute the DOA, is defined as

$$C(\varphi_S, i) = ce_{1i} = \frac{e_{1i}}{e_{11}}, \quad i = 2, 3, \cdots, M \tag{8}$$

As a result, based on one single active source, for any other azimuth angle, e.g., φ, the calibration value of the i-th channel can be determined by

$$C(\varphi, i) = C(\varphi_S, i)e^{jk(i-1)d(\cos\varphi - \cos\varphi_S)}, \quad i = 2, 3, \cdots, M \tag{9}$$

III. APM VERIFICATION

Similar to the use of a transponder, a standard antenna pattern measurement procedure was performed to verify the efficience of the proposed SAM, in which the transmitting antenna moves counterclockwise around the receiving Yagi antenna array at x-y plane, collecting field data at intervals of 10^o from x-axis. Only the forward of the array was measured, i.e., $\varphi = 20^o, 30^o, \cdots, 160^o$. The receiving ULA includes 8 Yagi antennas, i.e., $M = 8$. The distance of transceiver antenna remained constant, e.g., the length of the transmitting antenna cable remained unchanged. Fig. 3 illustrates the typical echo spectrum of a single active signal, which is used to calculate the calibration value through (9). LFM transmitting waveform was set with centre frequency of 340 MHz (i.e., wavelength $\lambda = 0.88$ m), bandwidth of 15 MHz (i.e., range resolution $\Delta R = 10$ m) and power of 0 dBm. The length of the transmitting cable was 20 m, i.e., the active source was located at the second rangecell of the radar. The range spectrum of Fig. 3(a) confirms the echo signal at 20 m, with a SNR of about 70 dB. Fig. 3(b) describes the range-doppler spectrum, in which a strong signal is displayed

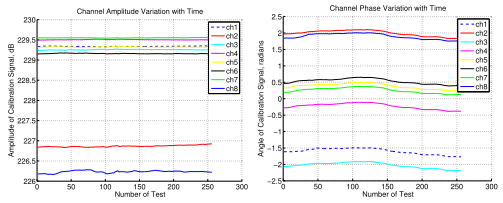

(a) Amplitude series (b) Phase series

FIGURE 4. Amplitude and phase variations of calibration source with 8 channels.

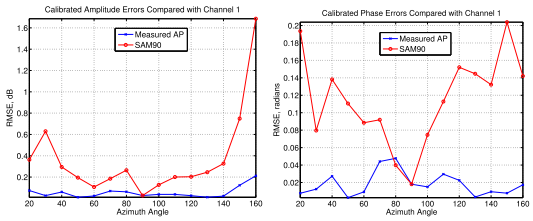

(a) Amplitude errors (b) Phase errors

FIGURE 5. Channel RMSE of amplitude and phase after calibration.

at zero doppler frequency because the transmitting antenna is static during the measurement at certain angle, i.e., no doppler shift is produced. Based on the measurement results, both the range and doppler spectra can be used for channel calibration, and they produce the same calibration value.

A number of active calibrations are conducted. Time series of amplitude and phase measurement of calibration signal at different receiving channels are shown in Fig. 4. Both the amplitude and phase remain stable with time, however, they vary with antenna channels, which show the necessity for channel calibration of antenna array. Ideally, the amplitude and phase of each channel remain equal after calibration, so the maximum array gain can be obtained. Fig. 5 shows the root mean square error (RMSE) of amplitude and phase after calibration at different azimuth angle. The calibrated amplitude and phase of channel 1 is set to the ground truth. The RMSE of calibrated amplitude and phase at each angle is calculated between the other antenna channels and channel 1. The blue cross line in Fig. 5(a) represents the amplitude errors, in which the channel amplitude is calibrated using the measured antenna pattern (AP) at different angles. The red circle line is the amplitude errors using the proposed SAM calibration based on the single measurement results at azimuth angle 90^o. The RMSEs of the SAM method for channel amplitude in Fig. 5(a) is slightly worse than those of the measured AP, however, as the RMSEs are within 1.6 dB (i.e., < 3 dB), it is acceptable for the channel variation. Fig. 5(b) shows the phase errors after calibration. The RMSEs of the SAM method for channel phase are within 0.2 radian or 11.5^o, which is smaller than the half power or 3 dB beam width of a standard 8-element linear array (i.e., 12.6^o) [29]. From Fig. 5(b), calibration using the measured AP achieves better performance on channel phase errors.

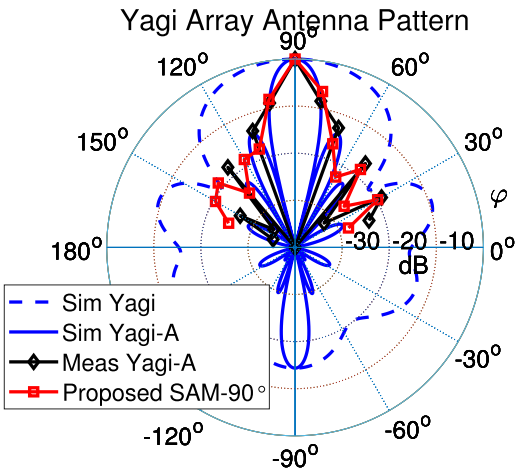

FIGURE 6. Yagi AP comparison of simulation and measurement.

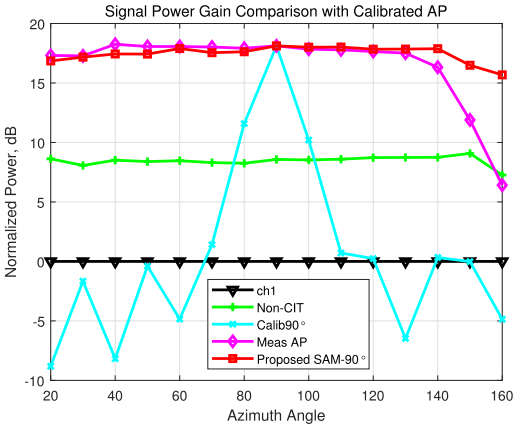

FIGURE 7. Power gain comparison with and without calibration.

In Fig. 6, the AP of the Yagi array shown in Fig. 1 obtained from different method is compared. The blue dotted line is a simulated AP of single Yagi antenna based on (3). The blue solid line is a simulated AP of Yagi array using (4). The black diamond line is the measured AP of Yagi array using standard APM procedure in which amplitude and phase error of array channels were calibrated based on (7) and (8) at fifteen discrete azimuth angles ranging from 20^o to 160^o. The red square line is the calculated AP of Yagi array using the proposed SAM in this paper based on measurement results at azimuth angle 90^o, i.e., $\varphi_S = 90^o$ in (8). So that $C(\varphi_S, i)$ is determined from (8), and the calibration values at other azimuth angle are calculated using Eq (9). As shown in Fig. 6, the measured AP of Yagi array agrees well with the simulated one. Even in the sidelobe region of the measured AP, clear peaks and nulls can be observed. This confirms that there is no obvious distortion in the pattern of the Yagi array. The AP obtained from SAM is alse consistent with the other two methods in the mainlobe, whereas there is slightly different in the sidelobe of AP, which does not affect the DBF performance. Although only the AP obtained based on the measurement results at $\varphi_S = 90^o$ is demonstrated in Fig. 6, the measurement results at any single angle are also available for AP calculation.

Fig. 7 illustrates the power gain comparison of signal with and without calibration referring a single channel power. The red square line is the DBF results of signal power at each azimuth angle after channel calibration by values from Eq (9) using SAM at $\varphi_S = 90^o$. The signal power at each angle obtained from SAM (and other methods) are normalized by the signal power of a single receiving channel at the same angle, e.g., channel 1 of the total 8 channels, shown as the black downward-pointing triangle line. The cyan cross line is the DBF result at $\varphi_S = 90^o$ (i.e., the other angles are not calibrated), which shows a good power gain (e.g., about 18 dB) at the calibrated direction, e.g., 90^o, but bad performance at other angles. The green plus sign line is the gain of 8-channel with non-coherent integration (NonCIT), which gets about 9 dB power gain at each angle. The magenta diamond line is the DBF results using the measured AP from $\varphi = 20^o - 160^o$. Both the red square and magenta diamond power are about 18 dB higher than the black line, which are in good agrrement with the theoretical value, e.g., $20\log_{10} 8 = 18$ dB, showing the availability of SAM calibration. The power gain from the measured AP (magenta diamond line) shows slightly instability at edge angles (e.g., $\varphi = 150^o, 160^o$) which may be due to inaccurate measurements at the edge of the array.

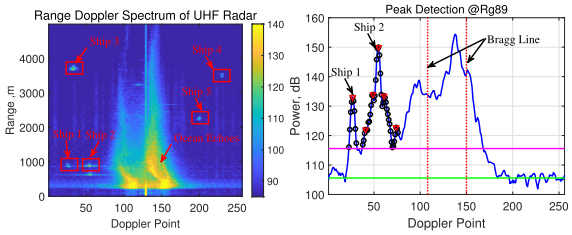

(a) Range-Doppler spec (b) Ship Peak Detection

FIGURE 8. Typical ship targets echoes of UHF radar.

IV. EXPERIMENT ANALYSIS

An offshore field experiment for coastal vessel detection (e.g., small fishing boat, motor boat etc.) in Taiwan Strait of Fujian Province, China, was carried out to verify the performance of SAM calibration. UHF radar worked in operation mode with FMICW waveform, centre frequency of 340 MHz, swept period of 40 ms, swept bandwidth of 15 MHz and peak power of 10 dBm, whose maximum detection distance was designed to be 5 km. The transmitting antenna was a Yagi antenna and the receiving antennas were 8 Yagi linear arrays. Typical ship targets echoes of UHF radar are shown in Fig. 8. Fig. 8(a) illustrates the range-Doppler (RD) spectrum of UHF radar, in which the x-axis represents Doppler frequency or the velocity of target with a velocity resolution of $\Delta v = 0.04$ m/s, and the y-axis represents range information with a range resolution of $\Delta R = 10$ m (i.e., there are 500 range cells). The colorbar represents the echo power in dB. The continuous and strong echo signals near the middle (e.g., velocity equals 0 at the 129th Doppler points) come from the Bragg scattering of ocean waves, which are potential to inverse sea state parameters, such as wind, wave and current. The discrete highlights

scattered in the graph represent ship targets, e.g., ship $1-5$ are marked, whose velocities are generally much greater than that of ocean currents. The Doppler spectrum of ship 1 and ship 2 at the same range cell (e.g., the 89th range cell or 890 m away from radar) are demonstrated in Fig. 8(b). The 27.5 dB and 44.7 dB SNR of ship 1 and ship 2,respectively, confirm the high quality of radar echoes. The green line represents the noise floor and the magenta line represents the detection threshold according to SNR (e.g., SNR $=$ 10 dB). A peak detection method is used to detect potential targets, e.g., the black circle marks in Fig. 8(b), among which the Doppler points of local maxima (e.g., the red downward-pointing triangle marks) are usually proposed subsequently.

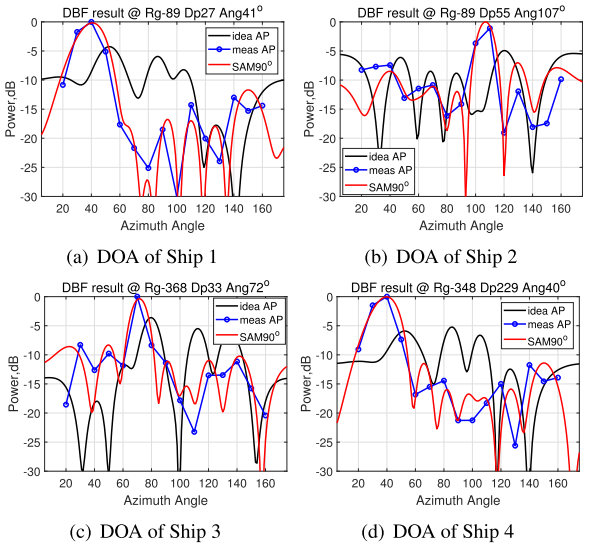

(a) DOA of Ship 1 (b) DOA of Ship 2

(c) DOA of Ship 3 (d) DOA of Ship 4

FIGURE 9. **DOA estimation of 4 ships with DBF of 8 Yagi array.**

As shown in Fig. 9, the DOA estimatons of DBF for ship targets are compared with different calibration method. The range cell (e.g., 89, or $89\times\Delta R = 890$ m away from radar) and Doppler point (e.g., 27, or $(27-129)\times\Delta v = -4.1$ m/s, radial velocity relative to radar) of potential ships are determined by peak detection. The x-axis represents azimuth angle φ from $5^o - 175^o$ with a resolution of 1^o as defined in Fig. 1. The y-axis is a relative power in dB to the maximum DBF power. The black line represents the DBF results of 8 Yagi arrays after receiving channel calibrated by simulated ideal antenna pattern (AP), i.e., the amplitude and phase errors of the radar receiving channels are uncalibrated. The blue circle line is the DBF results from calibration values of the measured AP using standard APM procedure in which calibration values are calculated at azimuth angle of $\varphi = 20^o - 160^o$ with a step of 10^o. The red line represents the DBF results using the proposed SAM calibration in this paper, in which calibration value at $\varphi = 90^o$ is measured by standard APM procedure, and those at other angles are determined from (9), with a step of 1^o. The DOA estimation results in Fig. 9 are not weighted by a sharp window function, with narrower main lobes near the normals line of array (e.g., $\varphi = 90^o$). Taking Fig. 9(a) as an example, there is no effective DOA estimation using ideal AP calibration, whereas both the DOA estimations of the measured AP calibration and SAM calibration are clear at $\varphi = 41^o$, e.g., independent peak with a certain SNR, and are in good agreement with each other, which indicates that the SAM calibration is effective. The same conclution can also be obtained from Fig. 9(b)- Fig. 9(d) that the DOA of different targets with different distances and velocities can be correctly estimated using SAM calibration, e.g., showing no difference with the results of the measured AP. In Fig. 10, the DOA estimation of ship 5 using SAM calibration at different angles is illustrated, agreeing well at $\varphi = 60^o, 90^o, 120^o$, which shows that the SAM calibration is independent of the active source angle, i.e., the azimuth angle of the single active signal can be user defined in APM mode of radar that is very convenient for field operating.

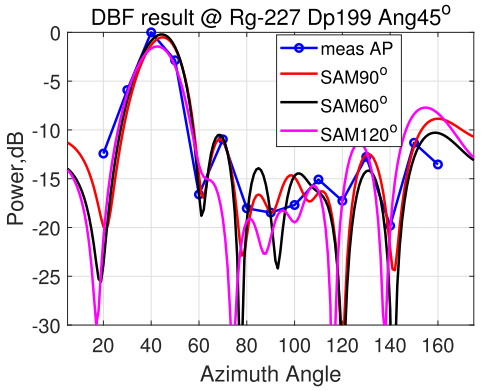

FIGURE 10. **DOA estimation of SAM calibration at different angle of single active source.**

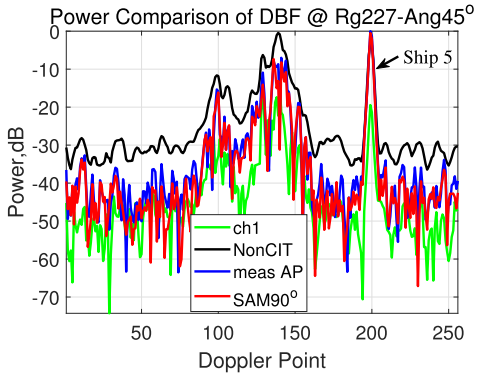

FIGURE 11. **Doppler spectrum power comparison of DBF with different calibration method.**

The DBF Doppler spectrum power comparison of ship 5 is shown in Fig. 11, in which the green line represents the Doppler spectrum of the receiving channel 1, the black line represents the Doppler spectrum of 8-channel with non-coherent integration (NonCIT), and the blue line and red line are the Doppler spectrum of DBF at the DOA of ship 5 (e.g., $\varphi = 45^o$) with measured AP calibration and SAM calibration respectively. Compared with channel 1, the Doppler power of DBF has a significant gain of about 20 dB, whereas the noise floor is also increased by about

TABLE 1. DBF gains of ship targets with different calibration method.

Method	Ship 1	Ship 2	Ship 3	Ship 4	Ship 5
Range (m)	890	890	3680	3480	2270
Angle (^{o})	41	107	72	40	45
Ch1 SNR (dB)	27.5	44.7	44.3	24	31.5
NonCIT (dB)	0.1	-0.2	-3.4	-1.8	-2.6
Ideal AP (dB)	7.4	4.6	4.1	5.9	4.1
Measured AP (dB)	10.7	7.3	4.2	10.6	9.9
SAM90^o (dB)	11.5	7.0	3.9	11.6	11.4

10 dB, i.e., a SNR increase of about $20 - 10 = 10$ dB is obtained after DBF processing, which is consistent with the performance of 8 arrays. Compared with the Doppler SNR of ship targets of channel 1, the SNR gain of DBF with different calibration method is summarized in Table 1. The SNR gains of SAM calibration, ranging from 3.9 dB to 11.6 dB (normalized by single channel SNR of Doppler power), are in good agreement with those of measured AP calibration, e.g., both achieving the ideal performance of 8 arrays, better than those of ideal AP calibration and NonCIT, stating that the proposed SAM calibration is successful. An interesting phenomenon can also be seen in Table 1 that targets with high SNR, e.g., 44.7 dB and 44.3 dB SNR of ship 2 and ship 3, respectively, get smaller SNR gain of DBF, e.g., 7 dB and 3.9 dB, respectively, whereas 27.5 dB SNR of ship 1 gets a high 11.5 dB SNR gain of DBF.

V. CONCLUSION

This paper introduces a UHF radar developed by Wuhan university of China for coastal ship target detection with the maximum detection distance of 5 km and a range resolution of 10 m. The range cell and and Doppler velocity of potential ship targets are determined by peak detection in the range-Doppler spectrum of radar. The DOA of target is estimated by DBF of 8 Yagi linear arrays. A practical calibration method based on single active source method (SAM) was proposed in this paper, which is very easy to deploy in field operating of radar. Different from the traditional antenna pattern measurement (APM) which requires a special designed transponder, the SAM method changes the receiver to the APM mode of radar to automatically calculate the channel calibration values of receier, in which the waveform, distance and power of the single active signal are user defined through the system soft of radar. The azimuth angle of the single active source is proved to be insignificant and could be optimized according to the field environment. A standard APM procedure at 15 azimuth angles from $\varphi = 20^o - 160^o$ with a step of 10^o was implemented to measure the AP of Yagi array for verifying the availability of the SAM calibration. It can be stated that the AP of Yagi array after SAM calibration is highly consistent with the measured AP and simulated ideal AP on the main lobe and most of the side lobes, except for a slight difference at the edge angle, which confirms the effectiveness of the proposed SAM method. The results of field experiment analysis show that the DOA estimations of DBF with SAM calibration are available for ship targets with different ranges and velocities, which agree well with DOA of the measured AP. The SNR gains of Doppler power spectrum ranging from 3.9 dB to 11.6 dB and depending on the SNR of targets, are obtained from DBF processing with SAM calibration, which are in good agreement with gains of the measured AP. As a result, the SAM calibration in this paper is proved to be convenient, practical, and effective for linear Yagi array.

Channel calibration is one of the most interesting technique in array radar signal processing and the basis of spatial spectrum estimation algorithms besides DBF, such as multiple signal classification (MUSIC) algorithm. For the running operation of radar, a simple and reliable calibration method is more important. The proposed SAM calibration in this paper provides a feasibility and idea for the practical and stable calibration of UHF linear array radar. However, the effect of antenna pattern distortion on the amplitude and phase errors of receiving channel is very complicated in the field environment. The antenna position errors, mutual coupling of array elements, and the surrounding electromagnetic environment, such as a vertical metal rod, an island or house shelter, interference radio, etc., all have a great impact on calibration performance. Perhaps a multi-auxiliary active source calibration approach provides a solution for such complex environments, but it's hard to control in field operating of radar. An experienced radar site deployment, such as a flat antenna field and a clean electromagnetic environment, is proved to greatly simplify the channel calibration process and avoid complex spatial spectrum estimation algorithms.

ACKNOWLEDGMENT

The authors would like to thank the Fujian Marine Forecasts, China, for providing the field experimental site.

REFERENCES

[1] J. T. Kohut and S. M. Glenn, "Improving HF radar surface current measurements with measured antenna beam patterns," *J. Atmos. Ocean. Technol.*, vol. 20, no. 9, pp. 1303–1316, Sep. 2003.
[2] Y. Lai, H. Zhou, Y. Zeng, and B. Wen, "Quantifying and reducing the DOA estimation error resulting from antenna pattern deviation for direction-finding HF radar," *Remote Sens.*, vol. 9, no. 12, p. 1285, Dec. 2017.
[3] X. Flores-Vidal, P. Flament, R. Durazo, C. Chavanne, and K.-W. Gurgel, "High-frequency radars: Beamforming calibrations using ships as reflectors," *J. Atmos. Ocean. Technol.*, vol. 30, no. 3, pp. 638–648, Mar. 2013.
[4] D. M. Fernandez, J. Vesecky, and C. Teague, "Calibration of HF radar systems with ships of opportunity," in *Proc. IEEE Int. Geosci. Remote Sens. Symp.*, Jul. 2003, pp. 4271–4273.
[5] H. Zhou and B. Wen, "Calibration of antenna pattern and phase errors of a cross-loop/monopole antenna array in high-frequency surface wave radars," *IET Radar, Sonar Navigat.*, vol. 8, no. 5, pp. 407–414, Jun. 2014.
[6] Y. Tian, B. Wen, J. Tan, and Z. Li, "Study on pattern distortion and DOA estimation performance of crossed-loop/monopole antenna in HF radar," *IEEE Trans. Antennas Propag.*, vol. 65, no. 11, pp. 6095–6106, Nov. 2017.

[7] R. Wang, B. Wen, and W. Huang, "A support vector regression-based method for target direction of arrival estimation from HF radar data," *IEEE Geosci. Remote Sens. Lett.*, vol. 15, no. 5, pp. 674–678, May 2018.
[8] B. M. Emery, L. Washburn, C. Whelan, D. Barrick, and J. Harlan, "Measuring antenna patterns for ocean surface current HF radars with ships of opportunity," *J. Atmos. Ocean. Technol.*, vol. 31, no. 7, pp. 1564–1582, Jul. 2014.
[9] C. Whelan, B. Emery, C. Teague, D. Barrick, L. Washburn, and J. Harlan, "Automatic calibrations for improved quality assurance of coastal HF radar currents," in *Proc. Oceans*, Oct. 2012, pp. 1–4.
[10] T. Updyke, "Antenna pattern measurement guide," Old Dominion Univ., Norfolk, VA, USA, Tech. Rep., Apr. 2018.
[11] Y. Tian, B. Wen, Z. Li, Y. Yin, and W. Huang, "Analysis and validation of an improved method for measuring HF surface wave radar antenna pattern," *IEEE Antennas Wireless Propag. Lett.*, vol. 18, no. 4, pp. 659–663, Apr. 2019.
[12] C. Whelan, M. Hubbard, D. Trockel, M. Daugharty, and H. Parikh, "Benefits of multiple antenna pattern measurement methods for maintaining a regional HF radar network," in *Proc. 4th ORCA*, 2018.
[13] L. Washburn, E. Romero, C. Johnson, B. Emery, and C. Gotschalk, "Measurement of antenna patterns for oceanographic radars using aerial drones," *J. Atmos. Ocean. Technol.*, vol. 34, no. 5, pp. 971–981, May 2017.
[14] G. Virone, A. M. Lingua, M. Piras, A. Cina, F. Perini, J. Monari, F. Paonessa, O. A. Peverini, G. Addamo, and R. Tascone, "Antenna pattern verification system based on a micro unmanned aerial vehicle (UAV)," *IEEE Antennas Wireless Propag. Lett.*, vol. 13, pp. 169–172, 2014.
[15] S. Wang, B. Wen, C. Wang, Z. Yan, K. Li, and J. Yang, "UHF surface dynamics parameters radar design and experiment," *IEEE Microw. Wireless Compon. Lett.*, vol. 24, no. 1, pp. 65–67, Jan. 2014.
[16] A. Paulraj and T. Kailath, "Direction of arrival estimation by eigenstructure methods with unknown sensor gain and phase," in *Proc. IEEE Int. Conf. Acoust., Speech, Signal Process. (ICASSP)*, vol. 10, Apr. 1985, pp. 640–643.
[17] B. Friedlander and A. J. Weiss, "Eigenstructure methods for direction finding with sensor gain and phase uncertainties," in *Proc. Int. Conf. Acoust., Speech, Signal Process. (ICASSP)*, vol. 5, Apr. 1988, pp. 2681–2684.
[18] E. K. L. Hung, "A critical study of a self-calibrating direction-finding method for arrays," *IEEE Trans. Signal Process.*, vol. 42, no. 2, pp. 471–474, Feb. 1994.
[19] Y. Shimada, H. Yamada, and Y. Yamaguchi, "Blind array calibration technique for uniform linear array using ICA," in *Proc. IEEE Region Conf. (TENCON)*, Oct. 2007, pp. 1–4.
[20] J. Kim, H. J. Yang, B. W. Jung, and J. Chun, "Blind calibration for a linear array with gain and phase error using independent component analysis," *IEEE Antennas Wireless Propag. Lett.*, vol. 9, pp. 1259–1262, 2010.
[21] T. McKelvey, "Auto-calibration of uniform linear array antennas," in *Proc. 27th Eur. Signal Process. Conf. (EUSIPCO)*, Sep. 2019, pp. 1–5.
[22] M. Asai and H. Arai, "Blind phase calibration by near field null detection for linear array antenna," in *Proc. Int. Symp. Antennas Propag. (ISAP)*, 2019, pp. 1–2.
[23] T. Helzel and M. Kniephoff, "Software beam forming for ocean radar WERA features and accuracy," in *Proc. OCEANS MTS/IEEE SEATTLE*, Sep. 2010, pp. 1–3.
[24] Y. Hou, B. Wen, Y. Tian, and J. Yang, "A uniform linear array self-calibration method for UHF river flow detection radar," *IEEE Antennas Wireless Propag. Lett.*, vol. 16, pp. 1899–1902, 2017.
[25] K. S. Kim, E. Yang, and N. H. Myung, "Self-calibration of an active uniform linear array using phase gradient characteristics," *IEEE Antennas Wireless Propag. Lett.*, vol. 18, no. 3, pp. 497–501, Mar. 2019.
[26] B. Liao, J. Wen, L. Huang, C. Guo, and S.-C. Chan, "Direction finding with partly calibrated uniform linear arrays in nonuniform noise," *IEEE Sensors J.*, vol. 16, no. 12, pp. 4882–4890, Jun. 2016.
[27] X. Zhang, Z. He, X. Zhang, and Y. Yang, "DOA and phase error estimation for a partly calibrated array with arbitrary geometry," *IEEE Trans. Aerosp. Electron. Syst.*, vol. 56, no. 1, pp. 497–511, Feb. 2020.
[28] L. Yang, Y. Yang, and J. Yang, "Robust adaptive beamforming for uniform linear arrays with sensor gain and phase uncertainties," *IEEE Access*, vol. 7, pp. 2677–2685, 2019.
[29] S. J. Orfanidis, *Electromagnetic Waves and Antennas*. Camden, NJ, USA: Rutgers Univ., 2010.
[30] Y. Wang, H. Chen, Y. Peng, and Q. Wan, *Spatial Spectrum Estimation Theory and Algorithm*. Beijing, China: Tsinghua Univ. Press, 2004.

CAIJUN WANG received the B.S. degree in radio physics, the M.S. degree in circuit and system, and the Ph.D. degree in signal processing from Wuhan University, Wuhan, China, in 2003, 2005, and 2008, respectively.

Since 2008, he has been with the Radar and Signal Processing Laboratory (RSPL), Electronic Information School, Wuhan University. His current research interests include radio frequency system design, test, and verification, ocean and river surface parameters remote sensing via HF/UHF radar, and radar data processing and applications.

YINGWEI TIAN (Member, IEEE) was born in Qianjiang, Hubei, China, in 1989. He received the B.Eng. and Ph.D. degrees from Wuhan University, Wuhan, China, in 2010 and 2015, respectively.

From 2015 to 2018, he was a Postdoctoral Fellow in geophysics with Wuhan University, where he is currently an Associate Researcher. His current research interests include ocean surface remote sensing via high-frequency ground wave radar and radar signal processing.

JING YANG was born in Xiangyang, Hubei, China, in 1983. She received the B.Eng. and Ph.D. degrees from Wuhan University, Wuhan, China, in 2005 and 2010, respectively.

She is currently a Lecturer in information and communication engineering with the School of Electronic Information, Wuhan University. Her current research interests include ocean surface remote sensing and signal processing.

HAO ZHOU (Senior Member, IEEE) was born in Macheng, Hubei, China, in 1978. He received the B.E., M.E., and Ph.D. degrees from Wuhan University, Wuhan, China, in 1999, 2001, and 2004, respectively.

He is currently a Professor with Wuhan University. His research interests include radar signal processing, adaptive signal processing, and the technology of high-frequency radar sea remote sensing.

BIYANG WEN was born in Xiantao, Hubei, China, in 1963. He received the B.Eng. degree from Shanghai Jiao Tong University, Shanghai, China, in 1983, and the M.S. and Ph.D. degrees from Wuhan University, Wuhan, China, in 1990 and 1997, respectively.

Since 1990, he has been with the School of Electronic Information, Wuhan University, where he is currently a Professor. His current research interest includes radio wave propagation and remote sensing of the ocean surface via high-frequency ground wave radar and UHF radar.

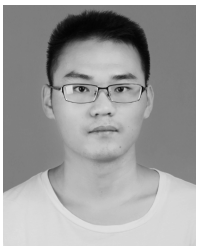

YIDONG HOU was born in Luan, Anhui, China, in 1992. He received the B.Eng. degree from Wuhan University, Wuhan, China, in 2015, where he is currently pursuing the Ph.D. degree.

His current research interest includes remote sensing of the ocean states and ocean-like rough surface scattering via UHF radar.